Published in final edited form as:
Biomaterials. 2013 May ; 34(14): 3729–3736. doi:10.1016/j.biomaterials.2013.02.008.

Functionalized Dendrimer-Based Delivery of Angiotensin Type 1 Receptor siRNA for Preserving Cardiac Function Following Infarction

Jie Liu[1,2], **Catherine Gu**[2], **E. Bernadette Cabigas**[2], **Karl D. Pendergrass**[2], **Milton E. Brown**[2], **Ying Luo**[1,2,*], and **Michael E. Davis**[1,2,3,*]

[1]Department of Biomedical Engineering, College of Engineering, Peking University, Beijing, China 100871

[2]Wallace H. Coulter Department of Biomedical Engineering at Emory University and Georgia Institute of Technology, Atlanta, GA 30322

[3]Division of Cardiology, Emory University School of Medicine, Atlanta, Georgia 30322

Abstract

Cardiovascular disease (CVD) is the leading cause of death throughout the world and much pathology is associated with upregulation of inflammatory genes. Gene silencing using RNA interference is a powerful tool in regulating gene expression, but its application in CVDs has been prevented by the lack of efficient delivery systems. We report here the development of tadpole dendrimeric materials for siRNA delivery in a rat ischemia-reperfusion (IR) model. Angiotensin II (Ang II) type 1 receptor (AT1R), the major receptor that mediates most adverse effects of Ang II, was chosen to be the silencing targeting. Among the three tadpole dendrimers synthesized, the oligo-arginine conjugated dendrimer loaded with siRNA demonstrated effective down-regulation in AT1R expression in cardiomyocytes *in vitro*. When the dendrimeric material was applied *in vivo*, the siRNA delivery prevented the increase in AT1R levels and significantly improved cardiac function recovery compared to saline injection or empty dendrimer treated groups after IR injury. These experiments demonstrate a potential treatment for dysfunction caused by IR injury and may represent an alternative to AT1R blockade.

Keywords

Dendrimer; Cardiomyocyte; Gene Expression; Ischemia-Reperfusion

*Co-Corresponding Authors: Michael E. Davis, Ph.D., Assistant Professor of Biomedical Engineering and Medicine, The Wallace H. Coulter Department of Biomedical Engineering, Emory University and Georgia Institute of Technology, 101 Woodruff Circle, Suite 2001, Atlanta, GA 30322, USA, michael.davis@bme.emory.edu, Telephone: (404) 727-9858, Fax: (404) 727-9873. Ying Luo, Ph.D., Associate Professor of Biomedical Engineering, Department of Biomedical Engineering, College of Engineering, Peking University, Room 206, Fangzheng Building, 298 Chengfu Road, Haidian District, Beijing 100871, China, ying.luo@pku.edu.cn, Telephone/Fax: +86 (10) 8252-9288.

1. Introduction

Cardiovascular disease (CVD) is the leading cause of death worldwide and with aging populations, incidence is on the rise. Myocardial infarction (MI) is class of CVD that accounts for 1 in every 6 deaths in the US alone, with roughly 1.5 million events annually [1]. Those that survive the initial insult, characterized by regional loss of tissue and function have a high probability of developing heart failure in subsequent years. With the global numbers on the rise, new treatments are greatly needed.

CVDs are controlled and influenced by numerous factors in the “cardiovascular continuum” [2,3]. One important hormone system involved is the Renin-Angiotensin-Aldosterone System (RAAS). The activation of RAAS following cardiovascular ischemic injury is supposed to promote blood pressure recovery, but its continuous stimulation can cause vasoconstriction, vascular and cardiac hypotrophy, and fibrosis [4]. Angiotensin II (Ang II), an octa-peptide hormone, which is the end-product of the RAAS, regulates most effects of RAAS [5]. It’s overexpression following MI leads to cardiomyocyte death and hypertrophy, vascular smooth muscle growth, and fibrosis, all of which cause adverse cardiac remodeling, progressive ventricular dysfunction, and finally heart failure [6]. Therefore, the inhibition of Ang II activation has become a common target for CVD therapy [7].

The Ang II type 1 receptor (AT1R) is the essential mediator of the well-known adverse effects of Ang II, and its activation results in worsened cardiac functions after injury [6, 8]. In contrast, the type 2 receptor (AT2R), another important receptor, is generally considered as a protective receptor, leading to improved function recovery [9–11]. By suppressing AT1R activity, the negative effects from Ang II could be reduced, while AT2R activity could be exacerbated, bringing more beneficial effects [12]. Currently, angiotensin receptor blockers (ARBs) are used following MI to restore blood pressure and possibly prevent fibrosis, and improve cardiac function in laboratories and in clinic [13–17]. Despite these interesting data, previous studies have shown that the suppression of AT1R at the gene expression level is superior to AT1R pharmacological blockade [18, 19], likely because the simple blockade interrupts the feedback loop in RAAS, causing renin and Ang II levels to increase in plasma, which may further activate the whole system. Such studies show a need for RNA interference (RNAi) therapeutics to selectively block receptor expressions following MI, specifically small interfering RNA (siRNA), one of the most efficient initiators of RNAi.

The development of siRNA delivery systems for cardiac tissue is one challenge that needs to be overcome for RNAi therapeutics to be successful in treating CVDs, as the non-phagocytic nature of cardiomyocytes set up a high barrier for the delivery of small RNA molecules. Bull et al. reported the usage of peptide-conjugated polymers for siRNA delivery in a cardiac myoblast cell line *in vitro*, but no *in vivo* efficiency was verified [20–22]. SiRNA-albumin conjugates have also been used in cardiac gene silencing *in vivo* by Lau et al., however a high dose (1–5 mg/kg) was required to induce a 40% silencing effect[23]. Due to the lack of efficiency, especially low efficiency *in vivo*, new delivery systems for cardiac tissue are highly in demand.

Among current non-viral delivery systems, dendrimeric materials have been regarded promising in siRNA delivery [24]. They are mono-disperse molecules and have tunable structures and properties. The rich cationic peripheries on dendrimers allow strong charge interaction with anionic siRNA molecules, forming stable particles to fight against nuclease digestion. Meanwhile, the buffering amines inside dendrimers can induce a unique “proton sponge” effect, which can trigger endosomal escape and release siRNA cargoes into cytoplasm. The inherent advantages of dendrimeric materials make them suitable for

constructing siRNA delivery systems; however their application in cardiac tissue has not been developed.

In this study, we aim to develop a non-cytotoxic and efficient "tadpole" siRNA delivery system for cardiac tissue based on dendrimeric materials, combining the strengths of a cationic dendrimer and a cell penetrating peptide (CPP) to enhance uptake by cardiomyocytes. Two types of CPPs, oligo arginine (R9) and TAT, were linked to the reduced thiol end to cystamine core G4.0 poly(amido amine) (PAMAM) through a polyethylene glycol (PEG) crosslinker, separately. This design allows the PAMAM moeity to regulate siRNA complexation and endosomal escape, CPP improves cell internalization, and the PEG segments and the disulfide linkage between the three parts should enhance biocompatibility. The properties and performance of the dendrimeric materials were first evaluated in isolated cardiomyocytes *in vitro*, and we chose AT1R as the target to exploit its potential cardiovascular application in a rat ischemia-reperfusion (IR) model.

2. Materials and methods

2.1 Synthesis of peptide-conjugated tadpole dendrimeric materials

To synthesize the tadpole dendrimeric material, reduced PAMAM dendrimer was reacted with dithiodipyridine functionalized PEG (Py-PEG-Py) and thiol-containing peptide, subsequently. 10 mg/ml cystamine core PAMAM G4.0 (Sigma) in PBS was reacted with dithiothreitol (DTT, Sigma) of 10 molar equivalents of disulfide bonds for 24 h at room temperature, and unreacted DTT was removed by 3k Da MWCO Amicon® Ultra Centrifugal Filters (Millipore). The reduced PAMAM was reacted with Py-PEG-Py (MW 2000, Jiaxing Biomatrix Inc.) of 5 molar equivalents of thiol groups for 24 h at room temperature, followed by extensive dialysis against deionized water using a cellulose membrane (7 kDa MWCO, Union Carbide) for 3 days to remove excess PEG. Cysteine terminated peptide R9 (Ac-CRRRRRRRRR-NH_2), TAT (Ac- CGGWRKKRRQRRR-NH_2) (GL Biochem Ltd), or cysteine (Sigma) of 1.5 molar equivalents of PEG was added to the intermediates obtained from above steps, and the reactions were allowed for 24 h. The crude product was purified by dialysis using a 10 kDa MWCO cellulose membrane and dried via lyophilization. The peptide modification level in each product was analyzed by ^{1}H-NMR (Figure 1B).

2.2 Gel retardation assay

To assess the siRNA complexation capability of dendrimeric materials, a gel retardation assay was conducted using siRNA loaded samples. SiRNA in PBS (2 μM) was added to an equal volume of dendrimer solutions of indicated concentrations to achieve varying N/P ratios, and the samples were incubated at room temperature for 20 min before loading in a 3.5% agarose gel in a pH 8.5 TBE buffer, and imaging by a Kodak Imaging System.

2.3 Particle size and zeta-potential

Dendrimers containing siRNA were prepared as described in 2.2 and diluted 10 times using deionized water. The sizes of the particles were analyzed through dynamic light scattering (DLS) experiments at an angle of 90° by a 90Plus Particle Size Analyzer instrument, and the zeta-potentials were measured through electrophoretic light scattering experiments by a Zeta Sizer Nano ZS90 instrument.

2.4 In vitro transfection in cardiomyocytes

Cardiomyocytes were isolated from 1 day-old Sprague–Dawley rat pups (Charles River Labs) as previously described [25] and cultured in Dulbecco's Modified Eagle Medium (DMEM; Cellgro) with 10% fetal bovine serum (FBS; Hyclone) and 1× penicillin–

streptomycin–glutamine (P/S/G, Cellgro) in 6-well plates until reaching 80% confluency. Dendrimeric material samples loaded with or without siRNA against AT1R (5′-UGAAGAGCCUGAUCAAAUA dTdT -3′ (sense) and 3′-dTdT ACUUCUCGGACUAGUUUAU- 5′ (antisense), Dharmacon) were prepared as described in 2.2 in DMEM with the minimal N/P ratios required to complex siRNA completely. The transfection was conducted in DMEM treatment medium (DMEM with 2% FBS and 1× L-glutamine) for 24 h. Total RNA was extracted using Trizol reagent according to the manufacturer's protocol and stored at −20°C prior to use.

2.5 Gene expression

cDNA reverse transcribed from total RNA by M-MLV kit (Invitrogen) was amplified by Power SYBR Green (Invitrogen) in an Applied Biosystems StepOne Plus real time PCR system with the following pairs of oligonucleotides: AT1R, TTCTCAATCTCGCCTTGGCTGACT (forward primer) and AAGGAACACACTGGCGTAGAGGTT (reverse primer); AT2R, AATATGCTCAGTGGTCTGCTGGGA (forward primer) and CACAACAGCAGCTGCCATCTTCAA (reverse primer); 18S, TTCCTTACCTGGTTGATCCTGCCA (forward primer) and AGCGAGCGACCAAAGGAACCATAA (reverse primer). Gene expression levels were normalized relative to that of the house keeping gene 18S, and the results were expressed as fold changes for siRNA loaded dendrimeric materials relative to siRNA unloaded dendrimeric materials (empty dendrimeric material treatment) for the *in vitro* transfection.

2.6 Animal studies

A randomized and double-blinded study consisting 4 groups (sham, IR + saline, IR + dendrimer, IR + dendrimer/siRNA) was conducted in a rat IR injury model. Adult Sprague-Dawley rats (Charles River Laboratories) were anesthetized with isoflurane (1–3%) followed by heart exposure, and the left descending coronary artery was occluded for a period of 30 min before releasing the suture. Immediately after reperfusion, 80 μl saline (IR group), or saline containing empty dendrimer (IR + dendrimer group), or saline containing dendrimer/siRNA particles (IR + dendrimer/siRNA group) were administrated by intramyocardial injection in 3 regions of the border zone as previously described. Dose of siRNA given was 5 μg/kg, or the corresponding mass of empty dendrimer. After injection, chests were closed and rats allowed to recover on a heating pad. All animal studies were approved by Emory University Institutional Animal Care and Use Committee.

At a 3-day time point, echocardiography and Pressure-Volume (PV) cardiac hemodynamics were conducted to evaluate functional changes, and data including stroke volume, end systolic volume, end diastolic volume, and ejection fraction (%) were collected. Following echocardiography and PV measurements, animals were sacrificed and left ventricle tissue was harvested and store at −80°C prior to use. Total RNA was extracted from the tissue using Trizol, and AT1R and AT2R copy number was determined by quantitative real-time PCR using a standard curve method and normalized to 18S.

2.7 Infarct size

To determine the infarct size after treatment, animals were divided into 3 groups: IR+ saline, IR+ dendrimer, and IR+ dendrimer/siRNA. Three days after injection, rats were anesthetized with inhaled isoflurane, and the coronary artery was re-occluded by suture at the same place of occlusion as the first surgery. The hearts were perfused with 50 μl of filtered 10% Evan's blue dye through the aorta until tissue beyond the ligated area became blue. After Evan's blue dye staining, hearts were sliced into 4 sections and soaked in 1% 2,3,5-triphenyltetrazolium chloride (TTC) solution for 15–20 min, followed by fixation in 4%

paraformaldehyde. Pictures were taken and ImageJ was used to trace the area of viable tissue (blue), area at risk (red), and infarcted area (white), with data being expressed as infarct area/area at risk.

2.8 Statistics

Quantitative results were presented as means ± SEM. Statistical comparisons were performed by one way analysis of variance (ANOVA) followed by the Tukey-Kramer post-test to compare selected data pairs using Graphpad Prism 3 Software. The level of significance was denoted by *, ** and ***, with P value set at <0.05, <0.01, and <0.005, respectively.

3. Results

3.1 Synthesis of peptide-conjugated tadpole dendrimeric materials

Figure 1A shows the structure of the tadpole dendrimeric materials. They consist of three parts: the cationic dendrimer head, the PEG crosslinker, and the peptide tail. The fan-shape dendrimer moiety was obtained from reducing cystamine core PAMAM G4.0, and the 32 positive charges on the surface provided siRNA binding sites with multivalent interactions. The PEG segment can partially shield the cationic charges on the particle to reduce the potential toxicity, and the flexibility of PEG also allows the peptide tails to interact with cell membrane with minimal steric hindrance. The conjugated CPPs are used to enhance cell uptake of siRNA loaded particles in cardiomyocytes. The disulfide bonds between the three parts enhance the material biodegradability and release siRNA in the reducing cytoplasm.

H^1-NMR spectra confirmed the conjugation of PEG and peptides to dendrimeric moiety (Figure 1B). The representative PEG peak (-OC$\boldsymbol{H}_2$C$\boldsymbol{H}_2$-) occurs in the 3.7–3.8 ppm range, the representative PAMAM peaks (–NCH$_2$C$\boldsymbol{H}_2$CO–) occur in the 2.4–2.6 ppm range, and the representative peak of the arginine residues (–HCCH$_2$C$\boldsymbol{H}_2$CH$_2$NH–) in the peptides occur in the 1.6–1.8 ppm range. Qualitative comparison between the peak area of PAMAM, PEG, and arginine showed nearly 100% modification of PEG to reduced end of PAMAM, and 81.8% and 80.0% peptide conjugation on each PAMAM molecular averagely for R9 and TAT, respectively.

3.2 Preparation of siRNA loaded particles

The complexation capacity of siRNA by tadpole dendrimers was evaluated by gel retardation assay. With increasing N/P ratios in the siRNA loaded samples, the amount of un-complexed siRNA decreased as the siRNA bands detected in gel electrophoresis became fainter when the N/P ratios were increased from 10 to 60. The siRNA bands disappeared when N/P ratios reached 60 in f-PAMAM-PEG and f-PAMAM-PEG-TAT, or 40 in f-PAMAM-PEG-R9 group (Figure 2), indicating the minimal N/P ratios that each tadpole dendrimer needs to complex all siRNA in the samples.

The diameters of siRNA loaded particles formed by tadpole dendrimers under the minimal required ratios were determined by DLS. The PAMAM G4.0, f-PAMAM-PEG, f-PAMAM-PEG-TAT, and f-PAMAM-PEG-R9 particles have diameters of 247±76 nm, 178±13 nm, 143±29 nm, and 302±20 nm, respectively (Figure 3 and Table 1). And the corresponding zeta-potentials of these particles were determined as 29.9±4.1 mV, 10.6±4.3 mV, 15.4±4.0 mV, and 3.2±0.6 mV.

3.3 siRNA transfection in isolated cardiomyocytes

Primary tests were conducted in the cardiomyoblast cell line H9C2 to detect the internalization of the tadpole dendrimers, and both TAT- and R9-conjuated dendrimers

showed their capabilities of delivering FITC-siRNA into cells (Supplemental Figure 1). To determine the transfection efficiency of tadpole dendrimers in cardiac cells, AT1R expression at the mRNA level in primary cardiomyocytes after siRNA delivery was detected by quantitative real-time PCR. Neonatal cardiomyocytes were isolated from one-day rat pups and treated with 100 nM siRNA in various particles for 24 h. No significant change in AT1R expression was observed in the f-PAMAM-PEG and f-PAMAM-TAT groups (120.8±24.9% and 96.7±9.6%, respectively), but the f-PAMAM-PEG-R9 group showed greater than 60% silencing effect compared to the control group (36.7±9.9%, $P<0.01$) (Figure 4). Since the oligo arginine conjugated tadpole dendrimer exhibited the most efficient delivery performance, the f-PAMAM-PEG-R9 was chosen for the animal experiments.

3.4 siRNA delivery in vivo

To determine the siRNA delivery efficiency of oligo-arginine-conjugated tadpole dendrimer *in vivo*, adult male rats were randomized into 3 treatment groups with injections of either saline alone (IR), or saline containing empty dendrimer (IR+ dendrimer), or saline containing dendrimer/siRNA particles (IR+ dendrimer/siRNA), followed IR injury ($n>6$ for each group, $N=36$ total). Sham animals were used for comparison. At 3-days following injury, the expression of AT1R at mRNA level increased significantly ($P< 0.05$) in IR group and IR+ dendrimer group by 1.92±0.26-fold and 2.01±0.37-fold, respectively, compared to sham rats. In contrast, the AT1R expression maintained a similar level (0.94±0.21 fold) as sham rats following siRNA delivery by tadpole dendrimer, significantly lower than IR injured group ($P<0.05$) (Figure 5A).

Additionally, AT2R expression level was examined in left ventricle tissue. There were slight decreases in IR group (0.74±0.20 fold) and IR+ dendrimer group (0.69±0.20 fold) compared to sham group, but neither was considered significant. In comparison, AT2R levels showed a trend to increase in IR+ dendrimer/siRNA group by 2.14±0.86-fold, but not to a significant degree (Figure 5B).

3.5 In vivo cardiac function

To determine if siRNA delivery against AT1R by the tadpole dendrimer could preserve cardiac functions post-IR, ejection fraction (EF), end systolic volume (ESV), and end diastolic volume (EDV) were determined from echocardiography and PV cardiac hemodynamics ($n>6$ for each group, $N=26$ total). Sham-operated rats had an EF of 74.3±2.7% that was significantly lower in IR group (56.3±2.4%, $P<0.005$) and IR+ dendrimer group (62.0±2.4%, $P<0.01$); however, the IR+ dendrimer/siRNA group demonstrated a significant improvement (71.9±1.9%, $P<0.005$ vs. IR, $P< 0.05$ vs. IR+ dendrimer), resulting in a similar ventricular function as the sham rats (Figure 6).

The ESV of IR group increased significantly (127.8±6.4 μl, $P<0.01$) compared to the sham group (76.0±6.4 μl), indicating a loss of ventricular contractility and increase in elasticity. While the empty tadpole dendrimer group showed no significant decrease (125.9±14.5 μl), the injection of the siRNA loaded dendrimer particles demonstrated a significant improvement (84.6±8.6 μl, $P< 0.01$ vs. IR, $P< 0.05$ vs. IR+ dendrimer) in ESV following IR injury (Figure 7A). A similar trend was observed in EDV, with EDV values of 222.1±18.1 μl in the sham group, and 250.2±12.8 μl, 263.7±10.2 μl, and 231.7±19.8 μl for IR, IR+ dendrimer, IR+ dendrimer/siRNA, respectively, but not to a significant degree (Figure 7B).

Infarct size was measured in different treatment groups using the gold standard TTC staining method 3d following injury. Data were expressed as infarct size/area-at-risk to ensure variations in risk area did not affect the results. As the representative images and grouped

data in Figure 8 demonstrate IR alone induced an infarct size of 47.8±4.8%. While there was no significant decrease in the IR+ dendrimer group (37.5±2.7%), the injection of dendrimer/siRNA particles significantly decreased infarct size to 18.4±3.1% ($P<0.005$ vs. IR, $P< 0.01$ vs. IR+ dendrimer) (Figure 8).

4. Discussion

CVDs are a leading cause of death worldwide and with an aging population and changing lifestyles, incidence is on the rise. Compared to traditional drugs, small RNA molecules, which initiate RNA interference (RNAi) in the cytoplasm, have great potential due to target sequence specificity and ease of design and synthesis. In addition, the RNAi mechanism regulates the targets at the gene expression level, usually leading to a loss of protein expression. Despite all the advantages of RNAi therapeutics its clinical use has not been fully exploited. Circulating RNA cannot readily enter cells and is subject to degradation by RNAses. Therefore, new delivery systems for RNAi therapeutics need to be developed.

Dendrimeric materials are promising candidates for siRNA delivery. One such material, PAMAM, has many advantages including high charge density and the ability for endosomal escape, leading to its successful *in vitro* and *in vivo* application in siRNA delivery to cell lines and tumor cells [24, 26]. We used a PAMAM moiety as the head of the tadpole to complex siRNA with a strong affinity due to the multivalent interactions, while the CPP at the tail served to enhance the internalization of siRNA loaded particles in cardiomyocytes. The PEG segment was introduced into the structure to reduce the potential toxicity from PAMAM [27–30] by partially shielding the cationic charges. With the PEG modification, the zeta-potential of f-PAMAM-PEG particles was nearly 3-fold lower than the particles formed by PAMAM G4.0. Similar decreases in zeta-potentials were also observed in the other two tadpole dendrimer particles. The drop in zeta-potential of R9 dendrimer particles is probably due to the smaller N/P ratio required by this material (40 for R9 dendrimer vs. 60 for unmodified or TAT dendrimer). Though numbers of studies have reported the toxicity of cationic PAMAM [31], no adverse effect from tadpole dendrimers in metabolic activity was detected in primary cardiomyocytes by MTT (Supplemental Figure 2), implying decreased cytotoxicity after modification. These results are consistent with studies showing that reducing the charge on PAMAM via modification results in reduced toxicity [25, 32].

With siRNA loading, PAMAM G4.0 (data not shown) and f-PAMAM-PEG failed to reduce the expression of AT1R, which implied that the charge interaction alone is not sufficient to translocate the particles into cardiomyocytes. CPPs, including oligo-arginine (R9) and TAT, have been used to enhance delivery efficiency in cardiac cells and myocardium [21, 33, 34]. In our study, the R9 conjugated tadpole dendrimer showed efficient siRNA delivery, but not the TAT conjugated dendrimer. As the TAT peptide also contains several arginines, it is unclear why it was not effective in delivering siRNA to cardiomyocytes while the R9 tadpole was. It is possible that the addition of lysine and phenylalanine residues creates a secondary structure different than that of R9. Furthermore, R9 contains more arginine residues and that may also be a potential mechanism. Additionally, the TAT particles (302±20 nm) were larger than R9 particles (178±13 nm), and the difference may also affect the transfection since smaller particles are easier to be internalized. While published studies from our laboratory show efficient cardiomyocyte internalization of nanoparticles up to 500 nm [25], the materials themselves were quite different and size cannot be ruled out.

Delivery of AT1R *in vivo* resulted in enhanced cardiomyocyte survival as evidenced by improved infarct size. While not directly measured, infarct size is indicative of cardiomyocyte necrosis/apoptosis and increased salvage of tissue leads to reductions in infarct size. There was no effect of the empty dendrimer, indicating the reduced infarct size

was a direct result of AT1R silencing. This is consistent with reports showing that AngII can induce cell death in cardiomyocytes [35, 36], as well as studies demonstrating angiotensin receptor blockers (ARBs) ability to reduce infarct size [37–39]. The reduction in infarct size was also supported by the improvements seen in cardiac function. IR injury significantly reduced cardiac function as measured by ejection fraction using invasive pressure-volume measurements. This was significantly improved by siAT1R delivery using the R9 tadpole. While 3 days is early to see changes in diastolic volume, end-systolic volume was increased by IR. This was also significantly improved by siAT1R delivery with the R9 tadpole, indicating improvements in systolic function. Additionally, R9 is not cardiomyocyte specific and enhanced delivery to other cell types cannot be ruled out. Prior studies from our laboratory showed that R9 can enhance uptake of microRNA to endothelial cells [25]. As AT1R is expressed in endothelial cells, delivery to other cell types may have contributed to AT1R reduction *in vivo* following intracardiac injection. Despite this, the changes seen *in vivo* were likely too early to be related to angiogenesis. Whether this improvement in cardiac function was sustained chronically was not examined. It is possible that chronic AT1R levels are not suppressed, or that other mechanisms may contribute to changes in chronic function. Studies to determine long-term effects of R9 tadpole delivery are underway, as well as studies to determine the length of gene suppression.

Angiotensin receptor blockers (ARBs) are used clinically to treat hypertension and improve post-infarction contractility. While beneficial in the affected tissue, global inhibition of AT1 following infarction may have unintended side effects in other tissues. Additionally, AngII can also bind to the AT2R, which has mostly beneficial effects [9–11]. Studies using ARBs have shown both increased and decreased levels of AT2R following treatment [39–41]. This response is dependent on the type of cell being studied, the time of detection, and the type of injury model. Yang et al. used antisense RNA to silence AT1R in an IR model in rat hearts, leading to a decrease in AT2R level [18], potentially mitigating some of the beneficial effects. In our study, after *in vivo* siRNA delivery, levels of AT2 were increased, though this was not considered statistically significant. Despite this, the levels were not reduced as in other studies and may contribute to the improvements seen with tadpole-mediated siRNA delivery. The synthesis of another important gene in regulating cardiac function, type 1 collagen (Col-1), is also increased upon Ang II activation [42]. In the present study, IR injury increased Col-1 levels and siAT1R tadpole-mediated delivery demonstrated a trend at reducing this (Supplemental Figure 3). It is possible that the 3-day time point is too early to see significant changes in this chronic fibrosis marker, or that mediators other than AngII may contribute to this *in vivo*. Finally, while AT1R is a promising target, it is not the only molecule involved in post-MI dysfunction. With the discovery of an increasing number of cardiac-specific microRNAs that can enhance cardiac regeneration [43–45], the R9 conjugated tadpole dendrimer may have further uses in drug delivery to improve the infarcted myocardium.

5. Conclusion

Our oligo-arginine-conjugated tadpole dendrimer is a non-cytotoxic and efficient non-viral delivery system for siRNA in cardiac tissue, and the delivery of siRNA against AT1R by the dendrimer was able to preserve cardiac function after ischemia-reperfusion injury in rats. The development of the tadpole dendrimer system may have potential for delivery of RNAi therapeutics to treat CVDs in the future.

Supplementary Material

Refer to Web version on PubMed Central for supplementary material.

Acknowledgments

The research was supported by the China Scholarship Council (JL). This publication has been funded in whole or in part with the Federal funds from the National Heart, Lung, and Blood Institute, National Institutes of Health, Department of Health and Human Services, under Contract No. HHSN268201000043C to MED, and the National Natural Science Foundation of China (Project No. 31170933) to YL.

References

1. Roger VL, Go AS, Lloyd-Jones DM, Benjamin EJ, Berry JD, Borden WB, et al. Heart disease and stroke statistics-2012 update a report from the American Heart Association. Circulation. 2012; 125:E2–E220. [PubMed: 22179539]
2. Dzau V, Braunwald E. Resolved and unresolved issues in the prevention and treatment of coronary artery disease: a workshop consensus statement. Am Heart J. 1991; 121:1244–63. [PubMed: 2008853]
3. Dzau VJ, Antman EM, Black HR, Hayes DL, Manson JE, Plutzky J, et al. The cardiovascular disease continuum validated: clinical evidence of improved patient outcomes: part I: pathophysiology and clinical trial evidence (risk factors through stable coronary artery disease). Circulation. 2006; 114:2850–70. [PubMed: 17179034]
4. Probstfield JL, O'Brien KD. Progression of cardiovascular damage: the role of renin-angiotensin system blockade. Am J Cardiol. 2010; 105:10A–20A. [PubMed: 20102883]
5. Dzau VJ. Theodore Cooper lecture: tissue angiotensin and pathobiology of vascular disease: a unifying hypothesis. Hypertension. 2001; 37:1047–52. [PubMed: 11304501]
6. Ferrario CM, Strawn WB. Role of the renin-angiotensin-aldosterone system and proinflammatory mediators in cardiovascular disease. Am J Cardiol. 2006; 98:121–8. [PubMed: 16784934]
7. Ma TK, Kam KK, Yan BP, Lam YY. Renin-angiotensin-aldosterone system blockade for cardiovascular diseases: current status. Br J Pharmacol. 2010; 160:1273–92. [PubMed: 20590619]
8. Harada K, Sugaya T, Murakami K, Yazaki Y, Komuro I. Angiotensin II type 1A receptor knockout mice display less left ventricular remodeling and improved survival after myocardial infarction. Circulation. 1999; 100:2093–9. [PubMed: 10562266]
9. Yang Z, Bove CM, French BA, Epstein FH, Berr SS, DiMaria JM, et al. Angiotensin II type 2 receptor overexpression preserves left ventricular function after myocardial infarction. Circulation. 2002; 106:106–11. [PubMed: 12093778]
10. Kaschina E, Grzesiak A, Li J, Foryst-Ludwig A, Timm M, Rompe F, et al. Angiotensin II type 2 receptor stimulation: a novel option of therapeutic interference with the renin-angiotensin system in myocardial infarction? Circulation. 2008; 118:2523–32. [PubMed: 19029468]
11. Ichihara S, Senbonmatsu T, Price E Jr, Ichiki T, Gaffney FA, Inagami T. Targeted deletion of angiotensin II type 2 receptor caused cardiac rupture after acute myocardial infarction. Circulation. 2002; 106:2244–9. [PubMed: 12390955]
12. Oishi Y, Ozono R, Yoshizumi M, Akishita M, Horiuchi M, Oshima T. AT2 receptor mediates the cardioprotective effects of AT1 receptor antagonist in post-myocardial infarction remodeling. Life Sci. 2006; 80:82–8. [PubMed: 17023005]
13. Cohn JN, Tognoni G. A randomized trial of the angiotensin-receptor blocker valsartan in chronic heart failure. N Engl J Med. 2001; 345:1667–75. [PubMed: 11759645]
14. Dahlof B, Devereux RB, Kjeldsen SE, Julius S, Beevers G, de Faire U, et al. Cardiovascular morbidity and mortality in the losartan intervention for endpoint reduction in hypertension study (LIFE): a randomised trial against atenolol. Lancet. 2002; 359:995–1003. [PubMed: 11937178]
15. Lithell H, Hansson L, Skoog I, Elmfeldt D, Hofman A, Olofsson B, et al. The study on cognition and prognosis in the elderly (SCOPE): principal results of a randomized double-blind intervention trial. J Hypertens. 2003; 21:875–86. [PubMed: 12714861]
16. Berthonneche, Corinne; Sulpice, Thierry; Tanguy, Stéphane; O'Connor, Stephen; Herbert, Jean-Marc; Janiak, Philippe, et al. AT1 receptor blockade prevents cardiac dysfunction and remodeling and limits TNF-α generation early after myocardial infarction in rats. Cardiovasc Drugs Ther. 2005; 19:251–9. [PubMed: 16193242]

17. Daniels MC, Keller RS, de Tombe PP. Losartan prevents contractile dysfunction in rat myocardium after left ventricular myocardial infarction. Am J Physiol Heart Circ Physiol. 2001; 281:H2150–8. [PubMed: 11668077]
18. Yang BC, Phillips MI, Zhang YC, Kimura B, Shen LP, Mehta P, et al. Critical role of AT1 receptor expression after ischemia/reperfusion in isolated rat hearts: beneficial effect of antisense oligodeoxynucleotides directed at AT1 receptor mRNA. Circ Res. 1998; 83:552–9. [PubMed: 9734478]
19. Voros S, Yang Z, Bove CM, Gilson WD, Epstein FH, French BA, et al. Interaction between AT1 and AT2 receptors during postinfarction left ventricular remodeling. Am J Physiol Heart Circ Physiol. 2006; 290:H1004–10. [PubMed: 16214839]
20. Nam HY, Kim JS, Kim SW, Bull DA. Cell targeting peptide conjugation to siRNA polyplexes for effective gene silencing in cardiomyocytes. Mol Pharm. 2012; 9:1302–9. [PubMed: 22452378]
21. Nam HY, Kim J, Kim S, Yockman JW, Kim SW, Bull DA. Cell penetrating peptide conjugated bioreducible polymer for siRNA delivery. Biomaterials. 2011; 32:5213–22. [PubMed: 21501867]
22. Nam HY, McGinn A, Kim PH, Kim SW, Bull DA. Primary cardiomyocyte-targeted bioreducible polymer for efficient gene delivery to the myocardium. Biomaterials. 2010; 31:8081–7. [PubMed: 20674007]
23. Lau S, Graham B, Cao N, Boyd BJ, Pouton CW, White PJ. Enhanced extravasation, stability and in vivo cardiac gene silencing via in situ siRNA-albumin conjugation. Mol Pharm. 2012; 9:71–80. [PubMed: 22141328]
24. Kesharwani P, Gajbhiye V, Jain NK. A review of nanocarriers for the delivery of small interfering RNA. Biomaterials. 2012; 33:7138–50. [PubMed: 22796160]
25. Gray WD, Che PL, Brown M, Ning XH, Murthy N, Davis ME. N-acetylglucosamine conjugated to nanoparticles enhances myocyte uptake and improves delivery of a small molecule p38 inhibitor for post-infarct healing. J Cardiovasc Transl Res. 2011; 4:631–43. [PubMed: 21833815]
26. Xu QX, Wang CH, Pack DW. Polymeric carriers for gene delivery: chitosan and poly(amidoamine) dendrimers. Curr Pharm Des. 2010; 16:2350–68. [PubMed: 20618156]
27. Stasko NA, Johnson CB, Schoenfisch MH, Johnson TA, Holmuhamedov EL. Cytotoxicity of polypropylenimine dendrimer conjugates on cultured endothelial cells. Biomacromolecules. 2007; 8:3853–9. [PubMed: 18004811]
28. Mukherjee SP, Davoren M, Byrne HJ. In vitro mammalian cytotoxicological study of PAMAM dendrimers - towards quantitative structure activity relationships. Toxicol In Vitro. 2010; 24:169–77. [PubMed: 19778601]
29. Jain K, Kesharwani P, Gupta U, Jain NK. Dendrimer toxicity:let’s meet the challenge. Int J Pharm. 2010; 394:122–42. [PubMed: 20433913]
30. Hunter AC. Molecular hurdles in polyfectin design and mechanistic background to polycation induced cytotoxicity. Adv Drug Deliv Rev. 2006; 58:1523–31. [PubMed: 17079050]
31. Liu J, Gray WD, Davis ME, Luo Y. Peptide- and saccharide-conjugated dendrimers for targeted drug delivery: a concise review. Interface Focus. 2012; 2:307–24.
32. Waite CL, Sparks SM, Uhrich KE, Roth CM. Acetylation of PAMAM dendrimers for cellular delivery of siRNA. BMC Biotechnol. 2009; 9:38–47. [PubMed: 19389227]
33. Won YW, McGinn AN, Lee M, Bull DA, Kim SW. Targeted gene delivery to ischemic myocardium by homing peptide-guided polymeric carrier. Mol Pharm. 2012; 10:278–85. [PubMed: 23136850]
34. Ko YT, Hartner WC, Kale A, Torchilin VP. Gene delivery into ischemic myocardium by double-targeted lipoplexes with anti-myosin antibody and TAT peptide. Gene Ther. 2009; 16:52–9. [PubMed: 18701915]
35. Cigola E, Kajstura J, Li B, Meggs LG, Anversa P. Angiotensin II activates programmed myocyte cell death in vitro. Exp Cell Res. 1997; 231:363–71. [PubMed: 9087178]
36. Grishko V, Pastukh V, Solodushko V, Gillespie M, Azuma J, Schaffer S. Apoptotic cascade initiated by angiotensin II in neonatal cardiomyocytes: role of DNA damage. Am J Physiol Heart Circ Physiol. 2003; 285:H2364–72. [PubMed: 12919932]

37. Flynn JD, Akers WS. Effects of the angiotensin II subtype 1 receptor antagonist losartan on functional recovery of isolated rat hearts undergoing global myocardial ischemia-reperfusion. Pharmacotherapy. 2003; 23:1401–10. [PubMed: 14620386]

38. Jalowy A, Schulz R, Dorge H, Behrends M, Heusch G. Infarct size reduction by AT1-receptor blockade through a signal cascade of AT2-receptor activation, bradykinin and prostaglandins in pigs. J Am Coll Cardiol. 1998; 32:1787–96. [PubMed: 9822110]

39. Jugdutt BI, Menon V. AT1 receptor blockade limits myocardial injury and upregulates AT2 receptors during reperfused myocardial infarction. Mol Cell Biochem. 2004; 260:111–8. [PubMed: 15228092]

40. Jugdutt BI, Menon V. Upregulation of angiotensin II type 2 receptor and limitation of myocardial stunning by angiotensin II type 1 receptor blockers during reperfused myocardial infarction in the rat. J Cardiovasc Pharmacol Ther. 2003; 8:217–26. [PubMed: 14506547]

41. Nio Y, Matsubara H, Murasawa S, Kanasaki M, Inada M. Regulation of gene transcription of angiotensin II receptor subtypes in myocardial infarction. J Clin Invest. 1995; 95:46–54. [PubMed: 7814645]

42. Horio T, Nishikimi T, Yoshihara F, Matsuo H, Takishita S, Kangawa K. Effects of adrenomedullin on cultured rat cardiac myocytes and fibroblasts. Eur J Pharmacol. 1999; 382:1–9. [PubMed: 10556498]

43. Porrello ER, Mahmoud AI, Simpson E, Johnson BA, Grinsfelder D, Canseco D, et al. Regulation of neonatal and adult mammalian heart regeneration by the miR-15 family. Proc Natl Acad Sci U S A. 2013; 110:187–92. [PubMed: 23248315]

44. Eulalio A, Mano M, Dal Ferro M, Zentilin L, Sinagra G, Zacchigna S, et al. Functional screening identifies miRNAs inducing cardiac regeneration. Nature. 2012; 492:376–81. [PubMed: 23222520]

45. Jayawardena TM, Egemnazarov B, Finch EA, Zhang L, Payne JA, Pandya K, et al. MicroRNA-mediated in vitro and in vivo direct reprogramming of cardiac fibroblasts to cardiomyocytes. Circ Res. 2012; 110:1465–73. [PubMed: 22539765]

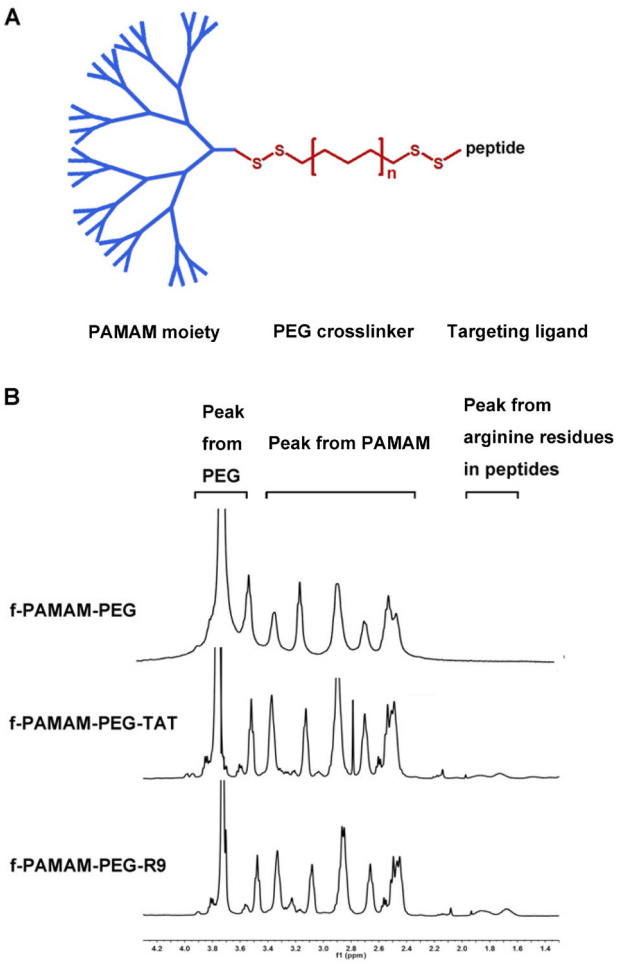

Figure 1. Tadpole design

The structure of the tadpole dendrimers (A) and the ^{1}H-NMR of the f-PAMAM-PEG, f-PAMAM-PEG-TAT, and f-PAMAM-PEG-R9 (B).

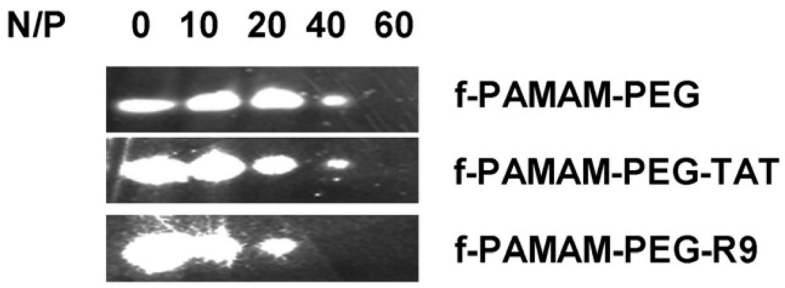

Figure 2. Gel retardation assay for siRNA complexation

Dendrimeric materials were mixed with siRNA at N/P ratios ranging from 10 to 60, and the un-complexed siRNA were detected in a 3.5% agarose gel in pH8.5 TBE buffer.

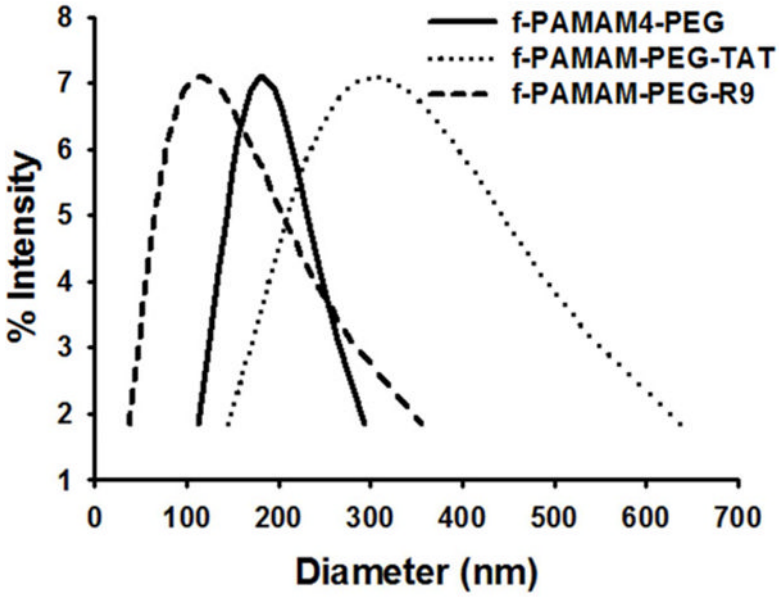

Figure 3. Analysis of particle size

The diameters of siRNA loaded tadpole particles analyzed by DLS at a scattering angle of 90°.

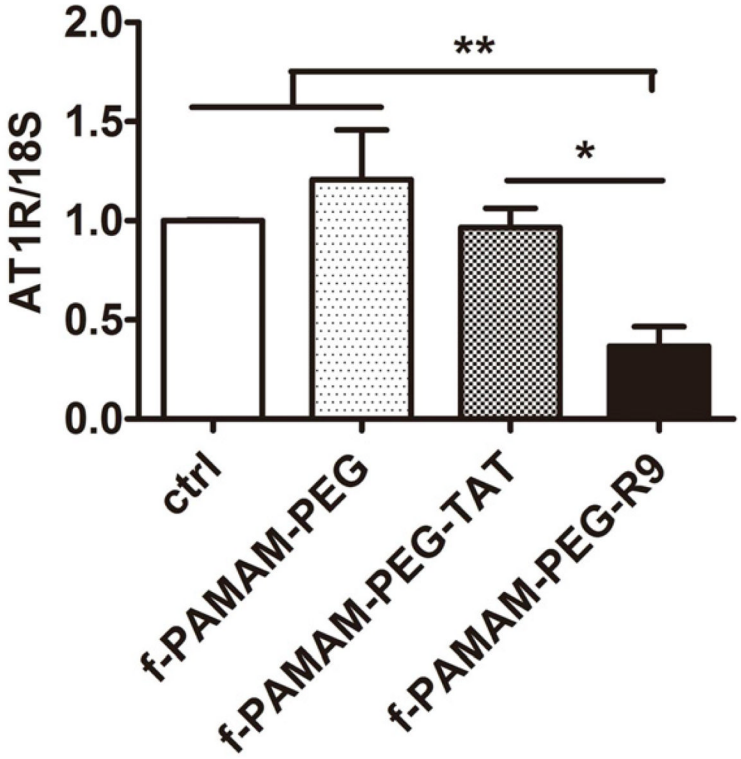

Figure 4. Efficacy of knockdown in primary cardiomyocytes

AT1R expression in isolated neonatal cardiomyocytes at 24 h following siRNA transfection with tadpole dendrimers. Gene expression was evaluated by real-time PCR using a ΔΔCT method, and the results were normalized to 18S expression (fold change) reported as mean ±SEM. n=3–4, *P<0.05, **P<0.01.

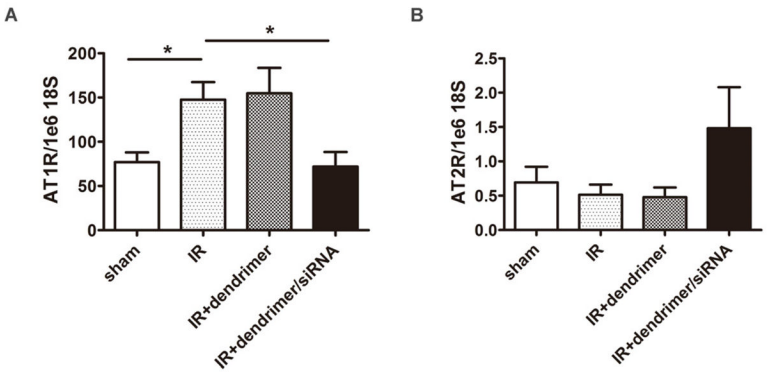

Figure 5. Angiotensin receptor expression in vivo

AT1R (A) and AT2R (B) expression in left ventricle tissue at the 3-day time point following IR injury. Gene expression was evaluated by real-time PCR using a standard curve method, and the results were normalized to 18S expression and reported as mean±SEM. $n>6$, $N=36$, $^{*}P<0.05$.

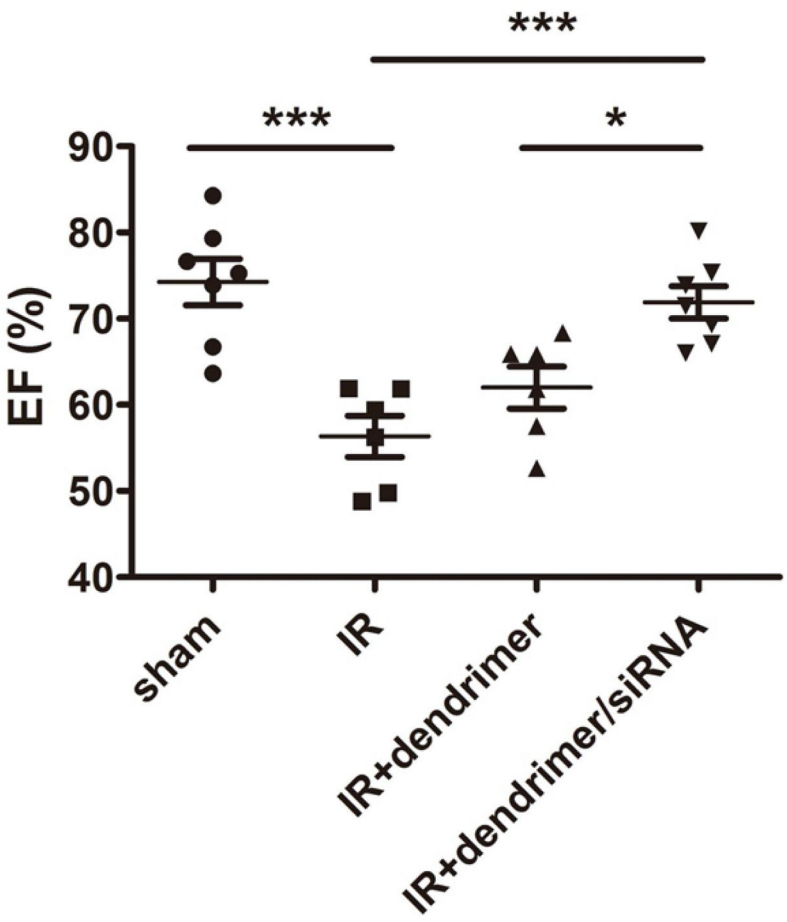

Figure 6. Cardiac function following dendrimer delivery

Ejection fraction (EF) of different treatment groups at the 3-day time point following IR injury. The results were reported as mean±SEM. $n>6$, $N=26$, $^{*}P<0.01$, $^{***}P<0.005$

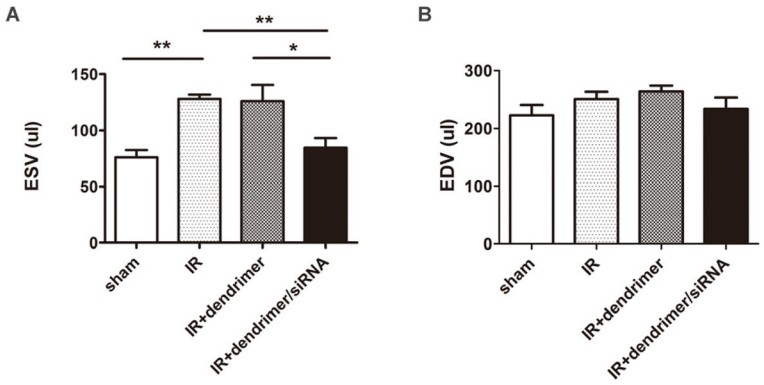

Figure 7. Invasive hemodynamic measurements of volume

The end systolic volume (ESV) (A) and the end diastolic volume (EDV) (B) of different treatment groups the at 3-day time point following IR injury. The results were reported as mean±SEM. $n>4$, $N=21$, $^{*}P<0.05$, $^{**}P<0.01$.

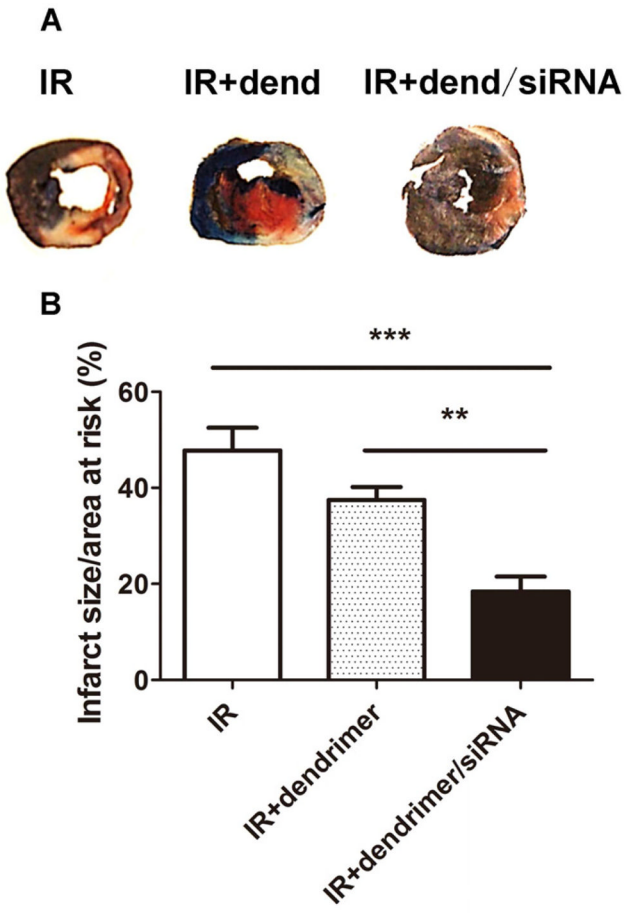

Figure 8. Assessment of infarct size

Representative images (A) and quantitation (B) of different treatment groups at the 3-day time point following IR injury. Viable tissue: blue, area at risk: red, infarcted area: white. The values of infarct size were calculated as infarct area/area at risk and presented as mean ±SEM. n=5, **P<0.01, ***P<0.005.

Table 1

Size and zeta-potential of siRNA loaded particles

Tadpole dendrimer	Diameter (nm)	Zeta-potential (mV)
PAMAM G4.0	247±76	29.9±4.09
f-PAMAM-PEG	178±14	10.6±4.35
f-PAMAM-PEG-TAT	302±20	15.4±4.01
f-PAMAM-PEG-R9	143±29	3.51±0.6